IMPACT MELT ENTRAINED IN BALLISTIC EJECTA OF LUNAR CRATERS V. J. Bray[1], N. Artemieva[2], C. D. Neish[3], A. S. McEwen[1] and J. McElwaine[2]. [1]The University of Arizona, Tucson, AZ, 85721. [2]Planetary Science Institute, Tucson, AZ, 85719. [3]NASA Goddard Space Flight Center, Greenbelt, MD, 20771. (vjbray@lpl.arizona.edu).

Introduction: One of the primary characteristics of impact crater formation is the generation and emplacement of melted target rock and ejected debris. It is generally accepted that the continuous impact ejecta blanket that surrounds impact craters is emplaced ballistically from material thrown out during the excavation stage of crater formation [1]. There are various hypotheses about melt emplacement: (1) ballistic ejection followed by additional flow after landing; (2) a ground-hugging flow during the later stages of crater modification which is deposited on top of the ejecta blanket [2]. Crater morphologies indicative of impact into still-molten ponds of impact melt, and the discovery of possible impact melt deposits flung far from their parent crater [3] point toward an intricate interplay between ejecta and melt. Terrestrial ejecta deposits are rare and poorly preserved, limiting our understanding of ejecta (and melt) emplacement.

We are surveying and analyzing the ejecta blankets of small fresh craters on the Moon to study the complex interaction of ejecta and impact melt and the degree of melt and ejecta mobility after the initial ballistic emplacement [4, 5]. We also seek to better link visual (LROC) and radar observations of impact melts, as some of the more degraded impact melts identified from LRO's Mini-RF data show less obvious melt morphology when inspected in visual imagery.

Method: We concentrate this study on simple craters so that ejected melt deposits remain primarily outside of the crater rim, rather than collecting behind terraces after the process of rim modification as noted in complex craters [6]. We also limit this study to the freshest of small craters, and identify candidate craters based on the retention of bright extensive rays.

Potential regions of exterior impact melt are identified using Mini-RF images (Fig. 1), where impact melt-rich deposits are characterized by particularly high (greater than 1.0) circular polarization ratios (CPR) [7]. The area was then surveyed using the high-resolution (~ 0.5-2 m/pixel) image coverage offered by the Lunar Reconnaissance Orbiter Narrow Angle Camera (LRO-NAC, [8]). Topographic profiles and slope information were extracted from the LRO WAC Global Lunar DTM 100 m (GLD100) [9] and the Lunar Orbiter Laser Altimeter (LOLA) slope data [10].

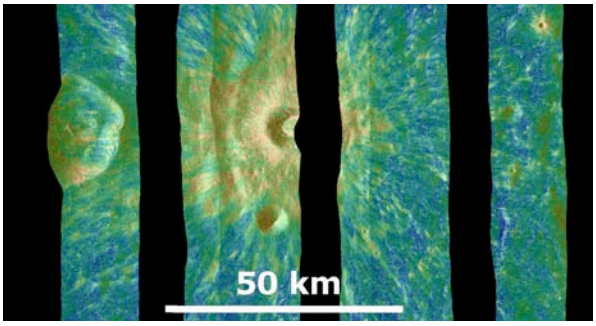

Figure 1: Mini-RF S-Band circular polarization ratio (CPR) data overlaid on same sense (SC) backscatter data. CPR values span the color spectrum from purple through red for values between 0 and 1.2. Blocky ejecta and impact melts are both characterized by large values of CPR (>1) and high radar backscatter.

Results: This abstract details the changes in ejecta and melt distribution with distance from the crater rim for a 9 km diameter simple crater at 259.7E, 3.25N. The visible ray system from this crater extends beyond 450 km from the crater rim and has a slight asymmetry. High CPR values in the mini-RF data (Fig. 1) are also noted to the west, suggesting a slightly oblique E→W impact. This rayed crater is typical of a lunar simple crater of its size, with a depth-diameter ratio of 0.2 and a wall slope slightly above 30 degrees [11].

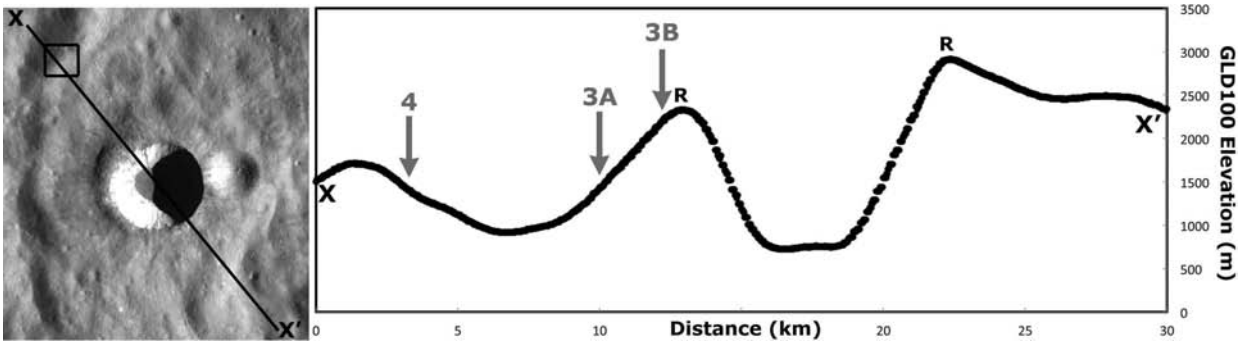

Figure 2: LRO WAC mosaic of the crater at 259.7E, 3.25N. The line through which a topographic profile has been extracted (using the GLD100) is shown from X to X'. The crater rim is marked 'R'. Melt and ejecta deposits shown in Fig. 3 are marked with grey arrows, the region shown in Fig. 4 is indicated with a boxed region on the image, and a grey arrow on the profile.

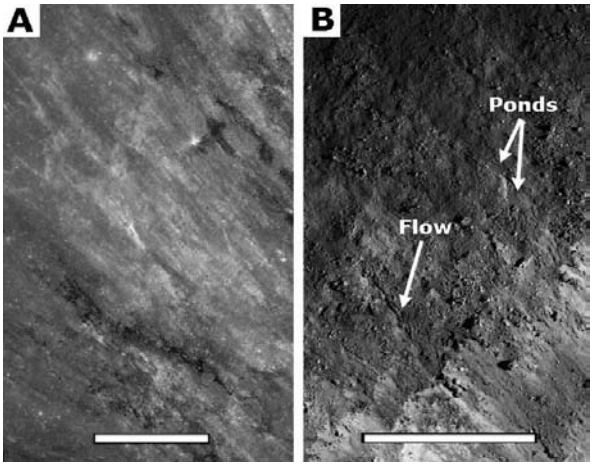

Figure 3: LROC NAC images of ejecta and melt deposits. A) Dark ejecta streaks lie on top of lighter toned ejecta (M109895309). B) Flows and ponds on the crater rim (M160607763). In both images North is up, the scale bar is 1 km and the crater is to the bottom right.

Close to the rim, dark deposits of impact melt are observed in ponds and channelized flows. This region of distinct melt extends < 2 km from the rim (Fig. 3B). At 2-6 km from the crater rim, the ejecta shows distinct high and low albedo streaks. The darker streaks are predominantly above the lighter-toned material (Fig. 3A). The continuous ejecta blanket of this crater extends to an average distance of 7 km from the crater rim, smaller than that expected for a crater of this size.

Beyond the edges of the continuous ejecta blanket, melt flows are still observed intermingled with ejecta up to 25 km away from the crater rim. Distinct flows emanate from beneath/within the ejecta (Fig. 4), and from low albedo deposits on top of lighter toned material. Unlike the flow/streak examples in Fig. 3, flows further from the crater occur on crater-facing slopes of more than 10° – too small a gradient for dry debris flows to form. The flows themselves are low albedo features when viewed in high-sun images (Fig. 4B).

The origin of the flow (marked as X on Fig. 4A) is 11 km away from the crater rim and appears to break out from within the ejecta deposit and flow back toward the crater down a slope of ~ 15 degrees for 1.2 km. At 11 km distance from the crater we would expect ejected material to strike the ground after a travel time from the crater of approximately 2 minutes, arriving with a speed of ~ 130 m/s (~ 200 m/s for the 25 km distant example). The most western flow shown in Fig. 4 has a volume of ~ 10^5 m^3. We do not know the size-frequency distribution of ejected melt - it may vary from small, mm-sized particles to tens of m blobs. Using a one-dimensional heat transfer equation, we predict that all particles larger than 10 cm remain liquid far in excess of their flight time [12]. It is not surprising then that the flow shown in Fig. 4 demonstrates a high degree of melt mobility after flight.

Conclusions: Our results indicate that impact melt, in addition to its emplacement as ponds/flows and sprays on top of near-rim ejecta, is incorporated into the ejecta blanket and emplaced ballistically (with some subsequent ground flow) at large distances from the crater. We note that these ejected melts tend to be low albedo and propose that many low albedo deposits around craters that show high CPR in radar data, are melt-rich, despite not showing any melt-like morphology. It is likely that most ejecta beyond the continuous ejecta blanket impacts the ground and continues to flow at speeds too high to allow the melt to settle out of the flow. The examples shown here include speeds of 130 and 200m/s. A ground-based flow of this speed would be turbulent and readily incorporate surface debris, both are factors that will lead to the rapid cooling of any entrained impact melt. The development of melt-like morphology (flows) of these melt-rich ejecta deposits requires the influence of high topography to impede the ejecta flow soon after it makes ground contact. This prevents vigorous mixing of the solid and molten debris, allowing the melt to separate out from the ejecta deposit and flow out toward lower elevation.

References: [1] Oberbeck (1975) Rev. Geophys. Space Phys. 13:337. [2] Osinski et al. (2011) EPSL 310:167. [3] Robinson et al. (2011) LPSC #2511. [4] Bray et al. (2010) GRL 37:L21202 [5] Denevi et al. (2012) Icarus 219:665. [6] Stoeffler et al. (2002) M&PS 37:1893. [7] Carter et al. (2012), JGR 117:E00H09. [8] Robinson et al. (2010) Space Sci. Rev. 150:81. [9]Scholten et al. (2011) LPSC #2046. [10] Smith et al. (2010) Space Sci. Rev. 150:209. [11] Pike (1976) The Moon 15:463. [12] Artemieva et al. (2013) LPSC #1413.

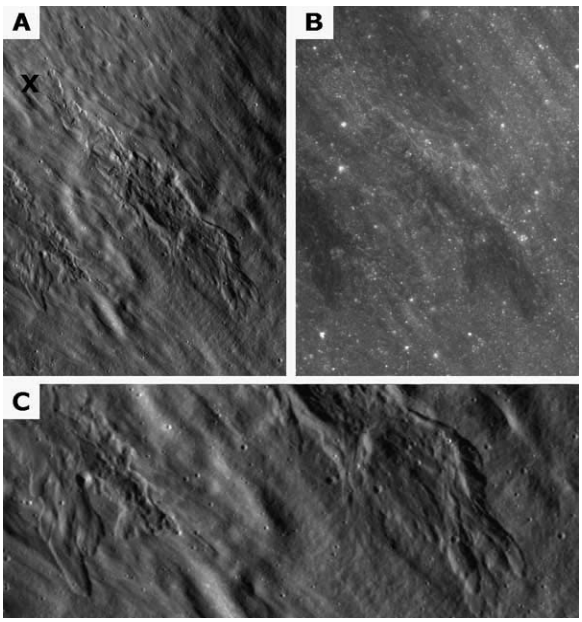

Figure 4: Ejected melt emanating from ejecta deposit 11km from the crater rim. A) Low sun (M102816150) and B) high sun (M109895309). C) Close up of the flow from image A. North is up in all images, and all images are 1 km wide.